

Differential Effects of Lysophosphatidylcholine on the Adsorption of Phospholipids to an Air/Water Interface

Samares C. Biswas,* Shankar B. Rananavare,^{†‡} and Stephen B. Hall*

*Departments of Molecular Biology & Biochemistry, Medicine, and Physiology & Pharmacology, Oregon Health & Science University, Portland, Oregon; [†]Department of Chemistry, Portland State University, Portland, Oregon; and [‡]Department of Computer Science and Electrical Engineering, OGI School of Science and Engineering, Beaverton, Oregon

ABSTRACT To determine how the hydrophobic surfactant proteins promote insertion of the surfactant lipids into an air/water interface, we measured the effect of lysophosphatidylcholine (LPC) on adsorption. Existing models contend that the proteins function either by disordering the lipids or by stabilizing a negatively curved structure located between the adsorbing vesicle and the interface. Because LPC produces greater disorder but positive curvature, the models predict opposite effects. With vesicles containing either dioleoyl phosphatidylcholine (DOPC) or the neutral and phospholipids isolated from calf surfactant, LPC increased the initial rate at which surface tension fell. The final surface tension, however, remained well above the value of ~25 mN/m expected for a saturated surface. With two preparations, dioleoyl phosphatidylethanolamine and gramicidin A-DOPC, which form the negatively curved hexagonal-II (H_{II}) phase and adsorb rapidly, LPC instead had little effect on initial adsorption but delayed the fall of surface tension below ~30 mN/m. LPC produced a similar inhibition of the late adsorption for extracted calf surfactant. Unlike dioleoyl phosphatidylethanolamine and gramicidin A-DOPC, small-angle x-ray scattering and ³¹P-nuclear magnetic resonance for extracted calf surfactant detected no evidence for the H_{II} phase. Our results indicate that although LPC can promote the initial adsorption of vesicles containing only lamellar lipids, it inhibits the facilitation by the hydrophobic proteins of late adsorption. Our findings support a model in which the surfactant proteins accelerate adsorption by producing a focal tendency to stabilize a negatively curved kinetic intermediate without a general shift to the H_{II} phase.

INTRODUCTION

In the lungs, pulmonary surfactant adsorbs quickly to the air/water interface. When a baby first creates the interface during its initial breath, pulmonary mechanics are normal within the first few respiratory cycles (1,2). For lungs in which prolonged ventilation at constant tidal volume has reduced surfactant function, a single deep inspiration, which expands the air/water interface and allows adsorption of fresh surfactant vesicles, restores normal pulmonary mechanics during the first exhalation (3). Adsorption therefore can form a film in situ at least within seconds.

Classical single-molecule surfactants and vesicles of pulmonary surfactant adsorb by processes that are fundamentally distinct. Classical surfactants adsorb as monomers, and increases in concentration above the critical micelle concentration (cmc) have little effect on adsorption. The low solubility of biological phospholipids makes determination of their cmc difficult, but the best estimates suggest that values are no higher than nanomolar (4) and probably lower. The dependence of adsorption on concentrations well above those levels suggests that pulmonary surfactant must insert into the interface as intact vesicles. Direct observation of adsorption confirms that conclusion (5,6).

Studies in vitro at concentrations below the levels in the lungs show that adsorption of vesicles containing the

surfactant lipids, without the proteins, is limited by an energy barrier to interfacial insertion. The process is considerably slower than if diffusion alone determined the rate (7). The dependence of kinetics on temperature indicates that an energy of activation is required to achieve adsorption (7,8). Several components of pulmonary surfactant increase the rate of adsorption, presumably by lowering that energy of activation. The hydrophobic surfactant proteins, and specifically SP-B, have the greatest effect (9). Other functions have been proposed for SP-B, including the ability to minimize collapse of compressed monolayers and to promote respreading of collapsed material into an expanding interface. SP-B's effect on adsorption, however, represents its best documented and most impressive function.

The consequences of ventilating lungs in the absence of SP-B suggest that the same energy barrier that limits adsorption in vitro is also present in vivo. Although patients (10) and mice (11) that congenitally lack functional SP-B have normal levels of surfactant lipids at the end of full-term pregnancies, they nonetheless develop the respiratory distress syndrome, in which the process of ventilation injures the thin epithelial barrier between capillary blood and alveolar air. In genetically modified adult animals, when production of SP-B stops, the lungs develop a similar injury (12). Dipalmitoyl phosphatidylcholine (DPPC), which forms metastable films that resist collapse during compression, functions poorly in premature infants (13) as a single-component therapeutic surfactant, presumably because of its slow rate of adsorption. These observations suggest that

Submitted May 26, 2006, and accepted for publication September 27, 2006.

Address reprint requests to Stephen B. Hall, Mail Code UHN-67, Oregon Health & Science University, Portland, OR 97239-3098. Tel.: 503-494-6667; Fax: 503-494-6670; E-mail: sbh@ohsu.edu.

© 2007 by the Biophysical Society

0006-3495/07/01/493/09 \$2.00

doi: 10.1529/biophysj.106.089623

rapid adsorption is not only characteristic of pulmonary surfactant but also physiologically essential.

Two mechanisms have been proposed to explain how different constituents promote adsorption. The original model suggests that factors such as the unsaturated phospholipids and the hydrophobic surfactant proteins disrupt ordered structures (14–16). Relative to other phospholipids, pulmonary surfactant contains an unusually high content of DPPC (17), which in single-component vesicles remains in the highly ordered gel ($L_{\beta'}$) phase at physiological temperatures. By disrupting the gel phase, different constituents would produce more fluid structures that might transform more rapidly from bilayer to interfacial film. More recent studies have shown that factors that can or should induce formation of the negatively curved hexagonal-II (H_{II}) phase also promote adsorption (18–20). These results support a second model in which constituents such as the surfactant proteins stabilize negatively curved structures, with a concave hydrophilic face, that bridge the gap between the vesicles and the interface, analogous to the stalk intermediate proposed as a crucial step in the fusion of two bilayers (21–23). Negative curvature and disordered lipids could of course both contribute to faster adsorption. The relative importance of the two characteristics, however, is uncertain and is significant both for the design of therapeutic surfactants and for understanding how pulmonary surfactant functions in the lungs.

Lysophosphatidylcholine (LPC) should have opposite effects on the two proposed mechanisms. LPC should produce more disorder (24–26), but it also forms structures with positive curvature, aggregating into micelles at lower concentrations and the hexagonal-I phase at higher levels (27). LPC should therefore promote adsorption if lipid disorder determines the kinetics but act as an inhibitor if negative curvature is more important. In the studies reported here, we first characterized the adsorption of vesicles containing only lipids and how LPC affected that process. We then confirmed that LPC inhibits adsorption of two preparations that form the negatively-curved hexagonal-II (H_{II}) phase and determined if LPC produces a similar inhibition of adsorption promoted by the hydrophobic surfactant proteins.

MATERIALS AND METHODS

Materials

Calf lung surfactant extract (CLSE), prepared as described previously (28), was provided by Dr. Edmund Egan (ONY, Amherst, NY). The complete set of neutral and phospholipids (N&PL) in CLSE were obtained by using gel permeation chromatography to remove the hydrophobic proteins (29). Previous studies have confirmed that the relative proportions of the different head groups, the fatty acid constituents, and cholesterol are the same in N&PL and CLSE (29,30).

Gramicidin A (GrA) from *Bacillus brevis* of $\geq 90\%$ purity was purchased commercially and used as received (Product 50845, Sigma-Aldrich, St. Louis, MO). Dioleoyl phosphatidylethanolamine (DOPE, Product 850725), dioleoyl phosphatidylcholine (DOPC, Product 850375), and egg LPC

(Product 830071), which contains predominantly saturated acyl chains, were obtained from Avanti Polar Lipids (Alabaster, AL), found to form a single spot on thin layer chromatography (31) and used without further purification. Dialysis used tubing (S41300-4, Fisher Scientific, Pittsburgh, PA) with a 4.8-nm-diameter pore and a cutoff of 12 kDa. Highly purified water obtained with a multicartridge system (Barnstead International, Dubuque, IA) was used throughout the experimental work. All other chemicals and solvents were analytical grade.

Methods

Preparation of lipid vesicles

Measurements of adsorption used samples prepared by two procedures designed to incorporate LPC either into both leaflets of the bilayer or preferentially into the outer leaflet. For incorporation into both leaflets, LPC was mixed in appropriate amounts with the other components in chloroform solutions. After complete mixing, the solvent was evaporated in round-bottomed test tubes under a stream of nitrogen. The resulting film was placed in a vacuum desiccator overnight to remove the last traces of solvent and then hydrated overnight with 10 mM HEPES, pH 7.0, 150 mM NaCl (HS), or in the case of N&PL and CLSE, with HS containing 1.5 mM $CaCl_2$ (HSC). The final concentration of phospholipid other than LPC, determined by assay of total phosphate (32), was 30 mM. The samples were then resuspended by several cycles of sequential heating to 50°C with vortexing for 3 min followed by cooling in an ice bath. The crude vesicles were dispersed further in a water-bath sonicator (model 3510, Branson, Danbury, CT) for 30 min. For incorporation of LPC into the outer leaflet, LPC was omitted from the original mixtures and then added as a micellar dispersion to the lipid vesicles. With both procedures, the vesicles with LPC were incubated overnight at 37°C before the kinetics of adsorption were measured.

Experiments to determine the effects of dialysis used 2-ml samples at 5 mM phospholipid dialyzed for at least 6 h against each of five successive changes of 1 liter of buffer. The diameter of the pores in the dialysis tubing was well below the hydrodynamic radius, determined by dynamic light scattering (DynaPro Light-Scattering Instrument, Proteins Solutions, Charlottesville, VA), of the dispersed aggregates with and without the highest dose of LPC (Table 1). Measurements of adsorption were conducted after dilution of the dialyzed sample to the appropriate concentration.

Measurements of surface tension

Surface tension was measured using a force transducer (KSV Instruments, Helsinki, Finland) attached to a 0.3-cm-wide Wilhelmy paper plate. Surface tension was recorded directly to a desktop computer using programs constructed with the graphical user interface LabVIEW (National Instruments, Austin, TX). The measurements used a Teflon beaker with a 4.0 cm² cross section in a fully humidified chamber maintained at 37.0 \pm 0.5°C with a circulating water bath. A fixed volume of 20 ml buffer, using HSC for CLSE and N&PL and HS for the other preparations, was added to the Teflon beaker, and after a stable temperature had been reached, 100 μ l of the dispersed vesicles at 30 mM non-LPC phospholipid was injected into the

TABLE 1 Hydrodynamic radii (nm) of particles in dispersed samples

LPC/PC (mol/mol)	0	0.25	0.30
DOPC	50.7 \pm 5.3	62.0 \pm 2.8	–
GrA-DOPC	138 \pm 3	76.5 \pm 5.2	–
N&PL	86.3 \pm 0.8	–	69.3 \pm 0.9
CLSE	144 \pm 12	–	114 \pm 3

The intensity of scattering prevented accurate measurements of hydrodynamic radii for samples with DOPE.

subphase to a final concentration of 150 μM . After gentle stirring for 15 min to provide complete mixing, experiments were begun by suctioning the film from the interface (7,8). Measurements of surface tension as a function of time are shown as representative curves to illustrate features that can be lost in averaged traces, with mean \pm SD for at least three experiments shown at selected points to indicate the variance of the data.

Small-angle x-ray scattering

Measurements of small-angle x-ray scattering (SAXS) from dispersions of CLSE used a home-built x-ray diffractometer. The x-ray generator (XRD-3000, Phillips, Almelo, The Netherlands) operates at 45 kV and 20 mA with a sealed fine-focus copper tube. The collimated monochromatic x-ray beam ($\lambda = 1.54 \text{ \AA}$) was produced using a β -nickel filter and a pinhole collimator. Lead stearate ($d = 49.8 \text{ \AA}$) was used as the calibrating standard. Measurements were performed on CLSE dispersions at 30 mM phospholipid sealed in glass capillaries (1 mm diameter) maintained at $37.0 \pm 0.2^\circ\text{C}$. The diffraction patterns were collected using a linear position-sensitive detector (spatial resolution of 92 mm/channel) interfaced to a personal computer through a multichannel analyzer (ND-53, Nuclear Data, Canberra Industries, Meriden, CT). Data were collected for each sample until the integrated intensity reached a common fixed value of 500,000 counts. The original data obtained as intensity versus channel number were converted to intensity versus q -spacing using the distances from sample to detector and from channel to the beam-stop, along with the wavelength of the x-rays. To correct for small differences in intensity caused by the different capillary tubes, each set of data was normalized with respect to the peak immediately adjacent to the beam-block that results from scattering in air.

Nuclear magnetic resonance

Proton-decoupled ^{31}P -NMR spectra from nonspinning dispersed samples of CLSE at 30 mM phospholipid were collected on a spectrometer (AMX-400, Bruker, Billerica, MA) using ^2H -NMR as an internal lock. Each spectrum was collected at a probe temperature of 37°C with 2000 scans at a 2-s repetition interval using a 15° pulse width and 100 kHz sweep width. A linewidth-broadening factor of 100 Hz was applied before Fourier transformation. Zero in the frequency domain corresponded to the chemical shift of phosphoric acid in D_2O .

RESULTS

Model lamellar lipids

Because of a prediction by one of the models, we used two methods to combine LPC with the other lipids. The hypothetical negatively curved structure between the vesicle and the interface would form from the outer leaflet of the bilayer. LPC confined to that outer leaflet should still inhibit adsorption. In one set of experiments, LPC was added to existing vesicles so that it would have access only to the external monolayer. LPC itself, however, is surface active and capable of lowering surface tension (Fig. 1). To ensure that changes in surface tension reflected adsorption of vesicles rather than free LPC, separate experiments used LPC dispersed together with the other lipids. Although this method of incorporating the compound allowed access to both sides of the bilayer, prior studies have shown that LPC distributes predominantly to the outer leaflet (33–42). The two protocols were therefore likely to produce similar vesicles.

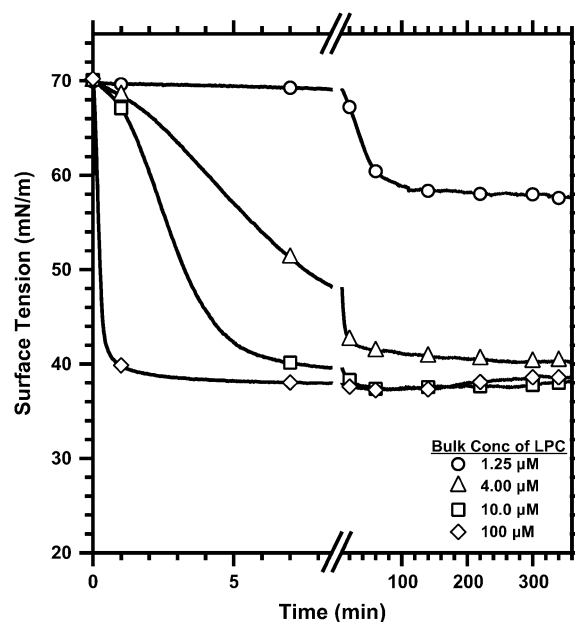


FIGURE 1 Adsorption of LPC. Curves show the variation of surface tension for individual experiments following removal of the interfacial film from above dispersions of LPC in HSC buffer at 37°C . Curves are representative of at least three experiments, with symbols at selected times to distinguish among different concentrations.

For all experiments, we also tested whether dialysis affected the kinetics of adsorption. The protocol for dialysis eliminated the ability to lower surface tension of samples containing only LPC. The concentration of samples containing only the other phospholipids, however, was unaffected. Dialysis therefore should have removed any free LPC but not LPC incorporated into vesicles.

LPC enhanced the initial reduction in surface tension of samples containing only lamellar phospholipids (Fig. 2). Vesicles of DOPC alone, without LPC, lowered surface tension slowly and to a limited extent, reaching only $63.1 \pm 0.5 \text{ mN/m}$ after 300 min (Fig. 2). LPC produced a dose-dependent increase in the rate at which surface tension fell and also lowered the final surface tension (Fig. 2). This faster reduction in surface tension occurred both when LPC was dispersed together with DOPC and when it was added subsequently to preformed vesicles. Dialysis had no effect. The final surface tension, however, remained well above the expected equilibrium spreading tension of $\sim 24 \text{ mN/m}$, at which films of phospholipids would saturate the interface (43). At the highest LPC/DOPC ratio of 0.25, surface tension reached only $46.6 \pm 0.3 \text{ mN/m}$ at 300 min. In the presence of LPC, adsorption of DOPC vesicles, although faster, remained incomplete.

LPC produced a similar effect with the N&PL obtained from extracted calf surfactant, CLSE, by using gel permeation chromatography to remove the hydrophobic surfactant proteins (29,30). LPC, whether dispersed together with the

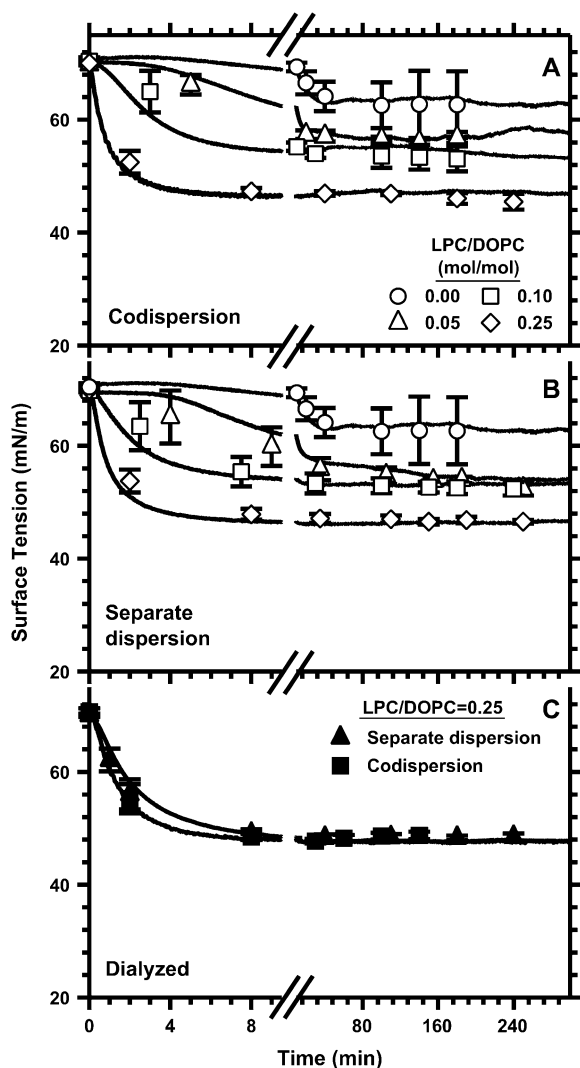


FIGURE 2 Effect of LPC on the adsorption of DOPC. Samples contained $150 \mu\text{M}$ DOPC in HS buffer at 37°C . Curves give the complete set of data for an individual experiment. Symbols give mean \pm SD for at least three experiments at selected times to indicate the variance of the data. (A) LPC and DOPC combined in organic solvent and dispersed together. (B) Dispersed LPC added to vesicles of DOPC. (C) Effect of dialysis on adsorption at the highest LPC/DOPC ratio.

N&PL or added to preexisting vesicles, produced a dose-dependent increase in the rate at which surface tension fell (Fig. 3). Dialysis had no effect. Like the samples of LPC-DOPC, adsorption was incomplete, and the final surface tension after 300 min remained $\geq 39 \text{ mN/m}$. LPC therefore produced similar effects on DOPC and N&PL, with faster initial adsorption that stagnated well before complete filling of the interface.

Lipids that form H_{II} structures

One premise of our studies was that LPC, which forms structures with positive curvature, would inhibit adsorption

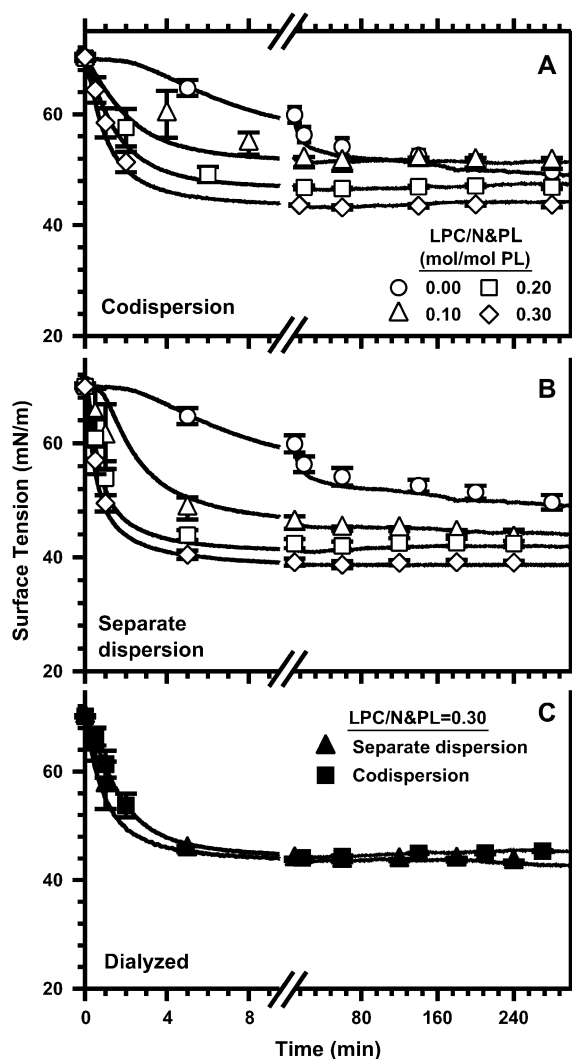


FIGURE 3 Effect of LPC on the adsorption of N&PL. Samples contained $100 \mu\text{M}$ phospholipid in HSC buffer at 37°C . Curves give the complete set of data for an individual experiment. Symbols give mean \pm SD for at least three experiments at selected times to indicate the variance of the data. (A) LPC and N&PL combined in organic solvent and dispersed together. (B) Dispersed LPC added to vesicles of N&PL. (C) Effect of dialysis on adsorption at the highest LPC/N&PL ratio.

of preparations that proceed via intermediates with negative curvature. Prior studies with two systems have shown that negatively curved structures produce faster adsorption. Both GrA-DOPC (20) and mixtures of lipids that contain phosphatidylethanolamine (PE), either as DPPC-PE or as DPPC-PE-phosphatidylglycerol (18,19), adsorb rapidly under conditions at which the negatively curved H_{II} phase is or should be present. In the current studies, before testing the effects of LPC on pulmonary surfactant, we first determined whether LPC would in fact inhibit adsorption by GrA-DOPC (0.07 mol/mol) and by DOPE.

DOPE without LPC adsorbed to the expected final surface tension of $\sim 24 \text{ mN/m}$ at rates too fast to distinguish features

of the adsorption isotherm (Fig. 4). LPC, whether added separately to the dispersed DOPE or mixed and then dispersed together, slightly delayed the initial decrease in surface tension. For both methods of combination, the LPC also introduced a plateau at an intermediate surface tension of ~ 44 – 55 mN/m (Fig. 4, A and B). The duration of the plateau depended on the amount of added LPC, extending beyond the 3-h length of the experiment for the highest LPC/DOPE ratio of 0.25 but terminating for lower amounts with a steepened slope until surface tension approached the expected final value of ~ 24 mN/m. With samples prepared by both methods for combining the lipids, the plateau persisted after dialysis (Fig. 4 C). Incorporation of LPC into the DOPE

structures therefore produced a minor effect on the initial fall in surface tension but inhibited adsorption below an intermediate surface tension.

LPC produced similar effects on adsorption of GrA-DOPC, which also adsorbs rapidly under conditions at which it forms H_{II} structures (20). Samples of GrA-DOPC, without LPC, adsorbed along isotherms that included a previously observed (20) distinct inflection point (Fig. 5). Surface tension fell at slowing rates to ~ 50 mN/m, but the slope then steepened. Added LPC had relatively little effect on the initial fall in surface tension or the late acceleration of

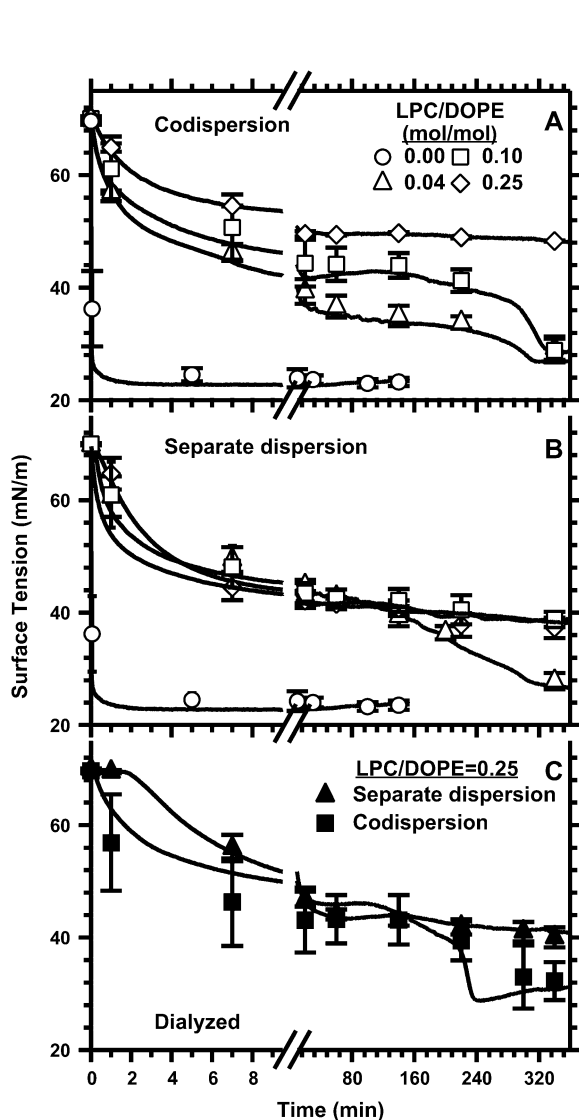


FIGURE 4 Effect of LPC on adsorption of DOPE. Curves show the variation of surface tension after removal of the surface film from a dispersion of $150 \mu\text{M}$ DOPE in HS buffer at 37°C . Curves are representative of at least three different experiments, with mean \pm SD shown at selected times. (A) LPC and DOPE dispersed together. Legend applies to panels A and B. (B) LPC added to DOPE after separate dispersion. (C) Effect of dialysis on adsorption of LPC-DOPE prepared by both methods of combination.

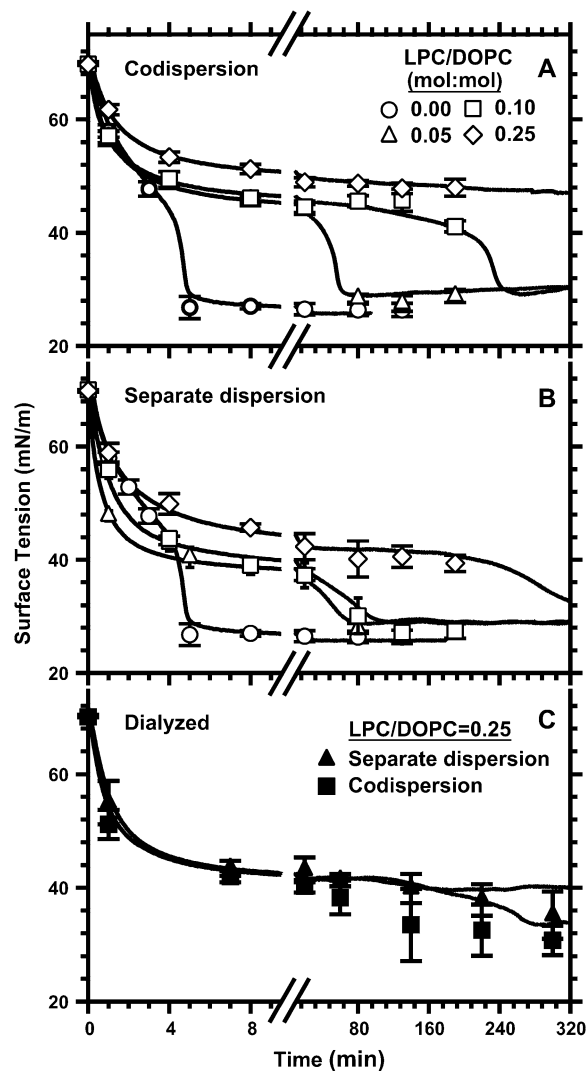


FIGURE 5 Effect of LPC on adsorption of GrA-DOPC (0.07 mol:mol). Curves show the variation of surface tension after removal of the surface film from a dispersion of $150 \mu\text{M}$ DOPC with GrA in HS buffer at 37°C . Curves are representative of at least three experiments, with mean \pm SD shown at selected times to indicate the variance of the data. Split time scale illustrates early as well as late events. (A) LPC dispersed along with GrA/DOPC. (B) LPC added to GrA/DOPC after separate dispersion. (C) Effect of dialysis on adsorption of LPC-GrA/DOPC dispersions prepared by both methods of combination.

adsorption, but it delayed the inflection point (Fig. 5). Consequently, LPC produced a dose-dependent prolongation of a plateau at intermediate surface tensions. Results were similar for the two methods of combination, and dialysis produced little change (Fig. 5 C). Like its effect on DOPE, LPC had little effect on the initial adsorption of GrA-DOPC but a major inhibition of the late acceleration.

Effect of surfactant proteins

Experiments with CLSE used the same two methods to incorporate LPC into bilayer vesicles. Samples containing only CLSE, without LPC, produced results similar to previously published studies (7,20,44). Surface tension fell at slowing rates to an inflection point at ~ 35 mN/m, after which the slope became steeper until surface tension reached a final value of ~ 24 mN/m (Fig. 6). LPC added by both methods had minimal effect on the initial fall in surface tension to ~ 40 – 45 mN/m, but it produced a dose-dependent delay in the inflection point and, therefore, a plateau at ~ 40 mN/m. Greater amounts of LPC produced little change in the surface tension of the plateau or in the slope of the final drop in surface tension. For the three doses of LPC, the isotherms after the plateau during the drop to their final surface tension were roughly parallel. Dialysis produced no significant changes (Fig. 6 C). LPC therefore produced alterations in the adsorption of CLSE that were similar to its effects on DOPE and particularly on GrA-DOPC, delaying the fall in surface tension below an intermediate surface tension of ~ 40 mN/m.

These results raised the possibility that, like DOPE and GrA-DOPC, the surfactant lipids with the hydrophobic proteins might form the H_{II} phase. Both SAXS (Fig. 7) and ^{31}P -NMR (Fig. 8) from CLSE detected only lamellar structures. Under the same conditions at which the samples adsorbed rapidly, the d -spacing of the two peaks in SAXS had the relative values of 1:2 expected for multilamellar vesicles (Fig. 7), and no intensity above baseline at the d_1/d_2 of 1.73 expected for the second-order diffraction peak from a hexagonal phase (45). ^{31}P -NMR did show the appearance of an isotropic peak, but the signal otherwise fit well to the shape expected for vesicles, without a component contributed by tubular structures (Fig. 8). In contrast to the preparations with PE and GrA, the hydrophobic proteins achieved their effect on adsorption without inducing a general shift to the H_{II} phase.

DISCUSSION

LPC inhibits the effects of surfactant proteins

The principal result of these studies is that LPC inhibits the ability of the surfactant proteins to promote adsorption of the surfactant lipids to equilibrium surface tensions. In the absence of the proteins, the surfactant lipids of N&PL adsorb only to intermediate surface tensions of ~ 45 mN/m, well

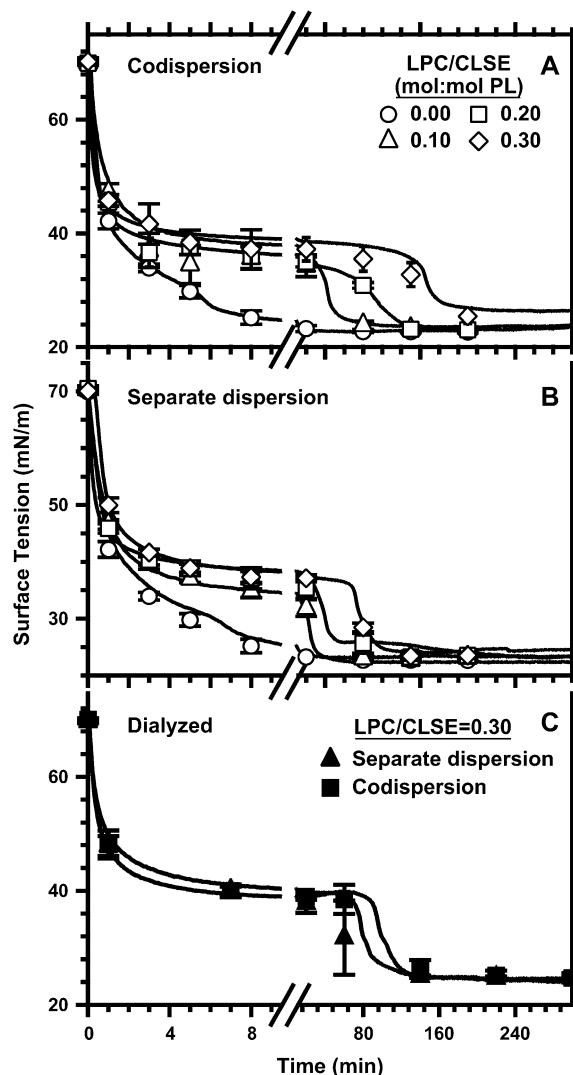


FIGURE 6 Adsorption of CLSE in the absence and presence of LPC. Curves show the variation of surface tension after removal of the surface film from a dispersion of $100 \mu\text{M}$ surfactant phospholipid at 37°C in HSC buffer. Curves are representative of three experiments under the same conditions. Symbols give mean \pm SD at specific times to indicate the variation among different experiments. (A) LPC and CLSE dispersed separately and then combined. (B) LPC and CLSE mixed and then dispersed together. (C) Samples prepared by both methods of combination and then dialyzed.

above the equilibrium level. The additional presence of the hydrophobic proteins in CLSE accelerates the initial fall in surface tension to ~ 45 mN/m, but they also produce an inflection point in the isotherm and a late acceleration (7). Despite a more crowded interface at lower surface tensions, adsorption occurs more rapidly below ~ 40 mN/m. LPC produces no discernible effects on the initial drop in surface tension, but it causes a dose-dependent delay in the inflection point. The slope of the final drop in surface tension remains approximately unchanged, and consequently, LPC produces a plateau at a roughly constant surface tension of ~ 35 – 40 mN/m. Despite the absence of any major effect on early

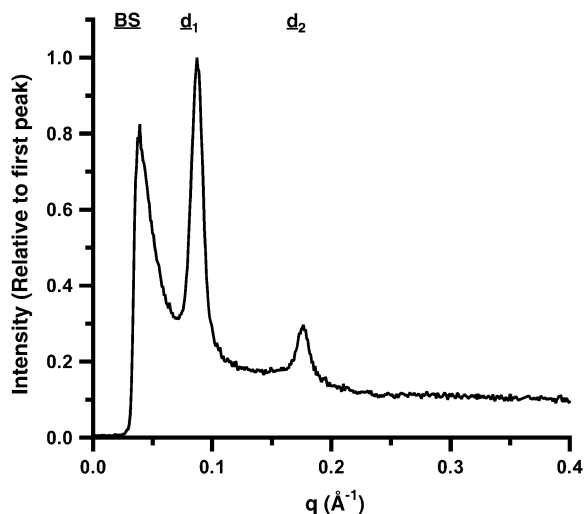


FIGURE 7 Small-angle x-ray scattering (SAXS) from dispersions of CLSE. Samples contained 30 mM phospholipid in HSC buffer at 37°C. Labels indicate peaks adjacent to the beam-stop (BS), and for first- (d_1) and second-order (d_2) diffraction.

adsorption, LPC inhibits the ability of the proteins to promote interfacial insertion of the vesicles to achieve a saturated film.

LPC similarly inhibits systems in which factors that induce negative curvature also promote adsorption. Both PE (18,19) and GrA (20) induce phosphatidylcholines to form the negatively curved H_{II} phase and to adsorb more rapidly. GrA, like the surfactant proteins, produces both a faster initial fall in surface tension and a late acceleration, so that DOPC, which alone stalls well short of the equilibrium spreading tension, will reach 24 mN/m. For both DOPE and

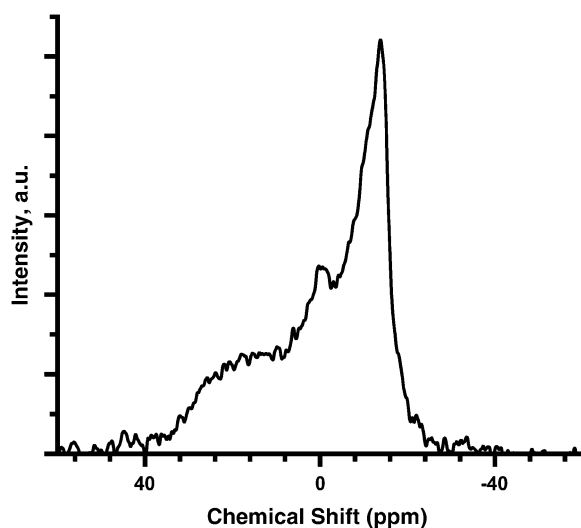


FIGURE 8 ^{31}P -NMR for dispersions of CLSE. Samples contained 30 mM phospholipid in HSC at 37°C.

GrA-DOPC, LPC inhibits the final fall in surface tension, and generates a plateau of dose-dependent duration at an intermediate surface tension. The inhibitory effects by the positively curved LPC are similar for adsorption promoted by the hydrophobic proteins and by the two factors known to produce negative curvature.

This observation adds to the chain of evidence concerning how the proteins facilitate adsorption. Although the role of the proteins during the subsequent unraveling of the surfactant aggregates is uncertain, their ability to promote adsorption when confined to the interface suggests that they facilitate at least the initial interaction of the vesicles with the surface. The similar (46) or equivalent (47) effects of factors in the vesicles and at the interface argue for a rate-limiting kinetic intermediate that is equally accessible from both locations. The ability of PE and GrA, which induce negative spontaneous curvature, to promote adsorption suggests that the kinetic intermediate might also be negatively curved. The similar effects of PE, GrA, and the hydrophobic surfactant proteins would then reflect a common stabilization of that rate-limiting structure. The similar kinetics, however, could nonetheless occur for processes that proceed along different pathways. The inhibition by LPC of adsorption promoted by factors with negative curvature and by the hydrophobic proteins provides additional support for the model in which the proteins stabilize a negatively curved structure intermediate between the interface and the vesicle.

In contrast to PE and GrA, the surfactant proteins promote adsorption without inducing formation of the H_{II} phase. Although with 17% (w/w) SP-B, ^2H -NMR does show changes in the structure of DPPC bilayers consistent with permanent curvature (48), for CLSE, with $\sim 1.5\%$ (w/w) hydrophobic protein, SAXS and ^{31}P -NMR detect only lamellar structures (Figs. 7 and 8). The absence of the H_{II} phase suggests that the effects of the proteins may be particularly focal, consistent with the ability of an individual SP-B to produce the full enhancement of adsorption (44). The proposed rate-limiting intermediate would require only a local effect where the vesicle contacts the interface. At the surface, the reduction in interfacial energy achieved by forming a film could permit structures that would be disallowed in the bulk subphase. The small amount of protein present in the surfactant mixture would then produce significant effects on their local environment and on rates of adsorption without causing a generalized phase transition.

A focal effect could be crucial in resolving the functional dichotomy faced by pulmonary surfactant. In the lungs, the surfactant lipids must adsorb rapidly to form the functional film but then avoid the reverse process of desorption when the decreasing alveolar surface area compresses the film during exhalation (49). The same global curvature that promotes rapid adsorption by preparations that form the H_{II} phase should destabilize the compressed film, limiting access to surface tensions below the equilibrium spreading values of ~ 24 mN/m. The PEs, for instance, which adsorb rapidly,

failed during compression to reach surface tensions much below equilibrium values (19). A more focal effect produced by the proteins could be more easily eliminated. The surfactant proteins and lipids, which are secreted together by the type II pneumocytes, separate at some point in the alveolus (50). If the separation occurs during compression of the adsorbed film, exclusion of the protein would eliminate the source of localized curvature, resulting in a more stable film.

Our studies used concentrations substantially lower than the levels present in the alveolus. This difference seems unlikely to alter the relevance of our findings to effects of the proteins in situ. The dependence of chemical kinetics on concentration is well known, and the adsorption of pulmonary surfactant in that respect is well behaved (7). Increased concentration could conceivably also change the nature of the lipid-protein aggregates by shifting the system to a different region of the phase diagram. Electron micrographs, however, of thin sections from the lungs indicate that water remains in excess (51,52). Free water should therefore coexist with the same hydrated phospholipid structures in vitro and in situ, with differences in concentration shifting the system along the tieline between those two phases. Although the higher concentrations in the lungs should produce quantitatively faster adsorption, the qualitative effects demonstrated here of the proteins and of LPC should remain valid in situ.

LPC promotes initial adsorption of the lipids

A second major finding is that LPC promotes the initial fall in surface tension for vesicles containing only lipids. For both DOPC and N&PL, LPC has minimal effect on the final surface tension, which remains >40 mN/m, well above the expected equilibrium levels. In both cases, however, LPC greatly increases the rate at which surface tension falls to that final value. LPC therefore produces opposite effects on early and late adsorption of the surfactant lipids, promoting the initial drop in surface tension but inhibiting the final approach to equilibrium, which requires the surfactant proteins.

We speculate that the different effects of LPC on early and late adsorption distinguish either two different pathways or two processes that affect progress along the same pathway. In either case, the importance of LPC's known effects on disorder and curvature would vary with surface tension. This variation would presumably reflect the different interfacial energies that provide the driving force for adsorption. The higher initial surface tension might then be adequate to drive adsorption that requires only disorder but insufficient for insertion into a denser film. Adsorption via a negatively curved structure would occur at all stages, and at lower surface tensions, with a reduced driving force, interfacial insertion could occur only by that mechanism. The two principal original models, which contend that factors promote adsorption by increasing disorder or by inducing negative curva-

ture, would then both be correct, although the effects of disorder would be evident only at higher surface tensions.

SUMMARY

In summary, LPC promotes the adsorption of vesicles that can reduce surface tension only to an intermediate value but inhibits adsorption to lower surface tensions by preparations that can form saturating films. These results, along with previous reports, suggest that adsorption involves initial insertion of vesicles into the interface by a process that requires only disordered lipids, and a later insertion into a denser film that must proceed via a structure with significant negative curvature, which is stabilized by the hydrophobic surfactant proteins and in particular by SP-B.

CLSE was provided by Dr. Edmund Egan (ONY, Amherst, NY).

These studies were funded by the National Institutes of Health (HL 54209).

REFERENCES

1. Enhorning, G., and B. Robertson. 1972. Lung expansion in the premature rabbit fetus after tracheal deposition of surfactant. *Pediatrics*. 50:58–66.
2. Lachmann, B., G. Grossmann, R. Nilsson, and B. Robertson. 1979. Lung mechanics during spontaneous ventilation in premature and fullterm rabbit neonates. *Respir. Physiol.* 38:283–302.
3. Nicholas, T. E., J. H. Power, and H. A. Barr. 1982. The pulmonary consequences of a deep breath. *Respir. Physiol.* 49:315–324.
4. Smith, R., and C. Tanford. 1972. The critical micelle concentration of ι - α -dipalmitoylphosphatidylcholine in water and water-methanol solutions. *J. Mol. Biol.* 67:75–83.
5. Sen, A., S.-W. Hui, M. Mosgrober-Anthony, B. A. Holm, and E. A. Egan. 1988. Localization of lipid exchange sites between bulk lung surfactants and surface monolayer: freeze fracture study. *J. Colloid Interface Sci.* 126:355–360.
6. Haller, T., P. Dietl, H. Stockner, M. Frick, N. Mair, I. Tinhofer, A. Ritsch, G. Enhorning, and G. Putz. 2004. Tracing surfactant transformation from cellular release to insertion into an air-liquid interface. *Am. J. Physiol. Lung Cell. Mol. Physiol.* 286:L1009–L1015.
7. Schram, V., and S. B. Hall. 2001. Thermodynamic effects of the hydrophobic surfactant proteins on the early adsorption of pulmonary surfactant. *Biophys. J.* 81:1536–1546.
8. King, R. J., and J. A. Clements. 1972. Surface active materials from dog lung. III. Thermal analysis. *Am. J. Physiol.* 223:727–733.
9. Wang, Z., S. B. Hall, and R. H. Notter. 1996. Roles of different hydrophobic constituents in the adsorption of pulmonary surfactant. *J. Lipid Res.* 37:790–798.
10. Noguee, L. M., G. Garnier, H. C. Dietz, L. Singer, A. M. Murphy, D. E. deMello, and H. R. Colten. 1994. A mutation in the surfactant protein B gene responsible for fatal neonatal respiratory disease in multiple kindreds. *J. Clin. Invest.* 93:1860–1863.
11. Clark, J. C., S. E. Wert, C. J. Bachurski, M. T. Stahlman, B. R. Stripp, T. E. Weaver, and J. A. Whitsett. 1995. Targeted disruption of the surfactant protein B gene disrupts surfactant homeostasis, causing respiratory failure in newborn mice. *Proc. Natl. Acad. Sci. USA.* 92:7794–7798.
12. Melton, K. R., L. L. Nesselin, M. Ikegami, J. W. Tichelaar, J. C. Clark, J. A. Whitsett, and T. E. Weaver. 2003. SP-B deficiency causes respiratory failure in adult mice. *Am. J. Physiol. Lung Cell. Mol. Physiol.* 285:L543–L549.

13. Chu, J., J. A. Clements, E. K. Cotton, M. H. Klaus, A. Y. Sweet, W. H. Tooley, B. L. Bradley, and L. C. Brandorff. 1967. Neonatal pulmonary ischemia. I. Clinical and physiological studies. *Pediatrics*. 40:709–782.
14. Meban, C. 1981. Effect of lipids and other substances on the adsorption of dipalmitoyl phosphatidylcholine. *Pediatr. Res.* 15:1029–1031.
15. Notter, R. H. 1984. Surface chemistry of pulmonary surfactant: the role of individual components. In *Pulmonary Surfactant*. B. Robertson, L. M. G. van Golde, and J. J. Batenburg, editors. Elsevier, Amsterdam, The Netherlands. 17–64.
16. Keough, K. M. W. 1985. Lipid fluidity and respiratory distress syndrome. In *Membrane Fluidity in Biology*, Vol 3. Disease Processes. R. C. Aloia and J. M. Boggs, editors. Academic Press, Orlando, FL. 39–84.
17. Brown, E. S. 1964. Isolation and assay of dipalmitoyl lecithin in lung extracts. *Am. J. Physiol.* 207:402–406.
18. Yu, S.-H., P. G. R. Harding, and F. Possmayer. 1984. Artificial pulmonary surfactant. Potential role for hexagonal H_{II} phase in the formation of a surface-active monolayer. *Biochim. Biophys. Acta.* 776:37–47.
19. Perkins, W. R., R. B. Dause, R. A. Parente, S. R. Minchey, K. C. Neuman, S. M. Gruner, T. F. Taraschi, and A. S. Janoff. 1996. Role of lipid polymorphism in pulmonary surfactant. *Science*. 273:330–332.
20. Biswas, S. C., S. B. Ranavavare, and S. B. Hall. 2005. Effects of gramicidin-A on the adsorption of phospholipids to the air-water interface. *Biochim. Biophys. Acta.* 1717:41–49.
21. Siegel, D. P., J. L. Burns, M. H. Chestnut, and Y. Talmon. 1989. Intermediates in membrane fusion and bilayer/nonbilayer phase transitions imaged by time-resolved cryo-transmission electron microscopy. *Biophys. J.* 56:161–169.
22. Kinnunen, P. K. 1992. Fusion of lipid bilayers: a model involving mechanistic connection to H_{II} phase forming lipids. *Chem. Phys. Lipids.* 63:251–258.
23. Chernomordik, L. V., E. Leikina, M. M. Kozlov, V. A. Frolov, and J. Zimmerberg. 1999. Structural intermediates in influenza haemagglutinin-mediated fusion. *Mol. Membr. Biol.* 16:33–42.
24. Lee, Y., and S. I. Chan. 1977. Effect of lysolecithin on the structure and permeability of lecithin bilayer vesicles. *Biochemistry*. 16:1303–1309.
25. Weltzien, H. U. 1979. Cytolytic and membrane-perturbing properties of lysophosphatidylcholine. *Biochim. Biophys. Acta.* 559:259–287.
26. Bhamidipati, S. P., and J. A. Hamilton. 1995. Interactions of lyso 1-palmitoylphosphatidylcholine with phospholipids: a ¹³C and ³¹P NMR study. *Biochemistry*. 34:5666–5677.
27. Fuller, N., and R. P. Rand. 2001. The influence of lysolipids on the spontaneous curvature and bending elasticity of phospholipid membranes. *Biophys. J.* 81:243–254.
28. Notter, R. H., J. N. Finkelstein, and R. D. Taubold. 1983. Comparative adsorption of natural lung surfactant, extracted phospholipids, and artificial phospholipid mixtures to the air-water interface. *Chem. Phys. Lipids.* 33:67–80.
29. Hall, S. B., Z. Wang, and R. H. Notter. 1994. Separation of subfractions of the hydrophobic components of calf lung surfactant. *J. Lipid Res.* 35:1386–1394.
30. Schram, V., and S. B. Hall. 2004. SP-B and SP-C alter diffusion in bilayers of pulmonary surfactant. *Biophys. J.* 86:3734–3743.
31. Touchstone, J. C., J. C. Chen, and K. M. Beaver. 1980. Improved separation of phospholipids in thin layer chromatography. *Lipids.* 15: 61–62.
32. Ames, B. N. 1966. Assay of inorganic phosphate, total phosphate and phosphatases. *Methods Enzymol.* VIII:115–118.
33. Kumar, V. V., B. Malewicz, and W. J. Baumann. 1989. Lysophosphatidylcholine stabilizes small unilamellar phosphatidylcholine vesicles. Phosphorus-31 NMR evidence for the “wedge” effect. *Biophys. J.* 55:789–792.
34. Kumar, V. V., W. H. Anderson, E. W. Thompson, B. Malewicz, and W. J. Baumann. 1988. Asymmetry of lysophosphatidylcholine/cholesterol vesicles is sensitive to cholesterol modulation. *Biochemistry*. 27:393–398.
35. Kumar, V. V., and W. J. Baumann. 1986. Bilayer asymmetry in lysophosphatidylcholine/cholesterol (1:1) vesicles. A phosphorus-31 NMR study. *Biochem. Biophys. Res. Commun.* 139:25–30.
36. Huang, C., and J. T. Mason. 1978. Geometric packing constraints in egg phosphatidylcholine vesicles. *Proc. Natl. Acad. Sci. USA.* 75: 308–310.
37. van den Besselaar, A. M., H. van den Bosch, and L. L. van Deenen. 1977. Transbilayer distribution and movement of lysophosphatidylcholine in liposomal membranes. *Biochim. Biophys. Acta.* 465: 454–465.
38. de Oliveira Filgueiras, O. M., A. M. van den Besselaar, and H. van den Bosch. 1977. Distribution of lysophosphatidylcholine in single bilayer vesicles prepared without sonication. *Biochim. Biophys. Acta.* 471: 391–400.
39. van den Besselaar, A. M., B. de Kruijff, H. van den Bosch, and L. L. van Deenen. 1979. Transverse distribution and movement of lysophosphatidylcholine in sarcoplasmic reticulum membranes as determined by ¹³C NMR and lysophospholipase. *Biochim. Biophys. Acta.* 555:193–199.
40. de Kruijff, B., A. M. van den Besselaar, and L. L. van Deenen. 1977. Outside-inside distribution and translocation of lysophosphatidylcholine in phosphatidylcholine vesicles as determined by ¹³C-NMR using (N-¹³CH₃)-enriched lipids. *Biochim. Biophys. Acta.* 465:443–453.
41. de Kruijff, B., P. R. Cullis, and G. K. Radda. 1976. Outside-inside distributions and sizes of mixed phosphatidylcholine-cholesterol vesicles. *Biochim. Biophys. Acta.* 436:729–740.
42. Wu, H., L. Zheng, and B. R. Lentz. 1996. A slight asymmetry in the transbilayer distribution of lysophosphatidylcholine alters the surface properties and poly(ethylene glycol)-mediated fusion of dipalmitoyl-phosphatidylcholine large unilamellar vesicles. *Biochemistry*. 35:12602–12611.
43. Yan, W., B. Piknova, and S. B. Hall. 2005. The collapse of monolayers containing pulmonary surfactant phospholipids is kinetically determined. *Biophys. J.* 89:306–314.
44. Schram, V., W. R. Anyan, and S. B. Hall. 2003. Non-cooperative effects of lung surfactant proteins on early adsorption to an air/water interface. *Biochim. Biophys. Acta.* 1616:165–173.
45. Luzzati, V. 1968. X-ray diffraction studies of lipid-water systems. In *Biological Membranes*. D. Chapman, editor. Academic Press, New York. 71–123.
46. Oosterlaken-Dijksterhuis, M. A., H. P. Haagsman, L. M. G. van Golde, and R. A. Demel. 1991. Interaction of lipid vesicles with monomolecular layers containing lung surfactant proteins SP-B or SP-C. *Biochemistry*. 30:8276–8281.
47. Walters, R. W., R. R. Jenq, and S. B. Hall. 2000. Distinct steps in the adsorption of pulmonary surfactant to an air-liquid interface. *Biophys. J.* 78:257–266.
48. Morrow, M. R., J. Stewart, S. Taneva, A. Dico, and K. M. Keough. 2004. Perturbation of DPPC bilayers by high concentrations of pulmonary surfactant protein SP-B. *Eur. Biophys. J.* 33:285–290.
49. Clements, J. A. 1977. Functions of the alveolar lining. *Am. Rev. Respir. Dis.* 115:67–71.
50. Wright, J. R., B. J. Benson, M. C. Williams, J. Goerke, and J. A. Clements. 1984. Protein composition of rabbit alveolar surfactant subfractions. *Biochim. Biophys. Acta.* 791:320–332.
51. Goerke, J. 1974. Lung surfactant. *Biochim. Biophys. Acta.* 344: 241–261.
52. Schürch, S., and H. Bachofen. 1995. Biophysical aspects in the design of a therapeutic surfactant. In *Surfactant Therapy for Lung Disease*. B. Robertson and H. W. Tausch, editors. Marcel Dekker, New York. 3–32.